COMPARATIVE TEST OF WIND LAWS FOR NUMERICAL WEATHER PREDICTION [1]

H. W. ELLSAESSER

Lawrence Radiation Laboratory, University of California, Livermore, Calif.

ABSTRACT

Six of the more common wind laws which have been used in numerical weather prediction were subjected to a comparative evaluation using the National Meteorological Center analyses of the WMO NWP Test Data November 29 to December 7, 1962. Specified winds were compared with observed wind analyses at initial times and 36-hr. barotropic forecasts were evaluated against verifying pressure heights. The linearized balance equation gave optimum results; the two major disadvantages of the balance equation are documented and spurious anticyclogenesis is shown to have a source in addition to the divergence of the advecting wind.

1. INTRODUCTION

The advent of NWP (Numerical Weather Prediction) intensified the concern of meteorologists with wind laws. As used herein the term wind law denotes a rule first for specifying the wind field (solenoidal or nondivergent component of the horizontal wind only) to be used in a numerical model and secondly for recovering the pressure height, z, from the horizontal wind. Note that the two transformations specified by a wind law are not necessarily inverses of each other. For simplicity specific wind laws will be referred to and defined by the upper case letter denoting the stream function (though not a true stream function in the quasi-geostrophic case) from which the horizontal wind may be determined by

$$\mathbf{V}=\mathbf{k}\times\nabla\psi. \tag{1}$$

Some half a dozen wind laws have been tested in the past 15 yr. At least three are currently used by operational NWP units indicating the absence of a convincing rationale for deciding among them. In an effort to develop such a rationale six of the more common and more promising wind laws were evaluated. The evaluation includes a survey of the advantages and disadvantages of each and an intercomparison of results obtained on actual data. The quantities compared are prescribed versus observed wind and forecast (barotropic) versus observed pressure height. All comparisons are based on NMC (National Meteorological Center at Suitland, Md.) analyses for the WMO NWP Test Data November 29 through December 7, 1962.

Wind laws considered are defined as follows:

G—Quasi-geostrophic

$$\nabla G\equiv g\nabla z/f, \quad \nabla^2 G\equiv g\nabla^2 z/f \tag{2}$$

P—Poor man's balance equation

$$\nabla P\equiv g\nabla z/f_0 \tag{3}$$

B—Balance equation

$$f\nabla^2 B\equiv g\nabla^2 z-\nabla B\cdot\nabla f-2J\left(\frac{\partial B}{\partial x},\frac{\partial B}{\partial y}\right) \tag{4}$$

L—Linearized balance equation

$$f\nabla^2 L\equiv g\nabla^2 z-g\nabla z\cdot\nabla f/f \tag{5a}$$

$$\equiv g\nabla^2 z-\nabla L\cdot\nabla f. \tag{5b}$$

(Although slightly different (5a) and (5b) are considered to be identical.)

$$L_E\equiv L \text{ (z, ellipticized by B)}$$

Q—Quasi-geostrophic vorticity

$$\nabla^2 Q\equiv g\nabla^2 z/f \tag{6}$$

O—Observed wind

$$\nabla^2 O\equiv\frac{\partial v}{\partial x}-\frac{\partial u}{\partial y}. \tag{7}$$

Two noninverse wind laws based on the observed winds were tested; O_B inverted by the balance equation (4) and O_L inverted by the linearized balance equation (5a) in the form which Shuman [17] called semi-geostrophic or S_2.

2. THE QUASI-GEOSTROPHIC WIND LAW, G

Despite the 40 percent mean vector deviation between the geostrophic and observed winds found by Neiburger

[1] This work was performed under the auspices of the U.S. Atomic Energy Commission.

295-999 O - 68 - 2

and Angell [14] and prior investigators, the geostrophic wind was and probably still is the most accurate universal wind law available. It was only natural that it should have been considered first for NWP. But the geostrophic wind has a divergence, $-\beta v_g/f$, unrelated to atmospheric divergence and which, when substituted into the two dimensional vorticity equation, cancels the beta term so that the equation no longer has Rossby waves as a solution. It also has a vorticity term, $\beta u_g/f$, which complicates inversion of the law to obtain pressure height.

As a solution to these and other problems, horizontal divergence was eliminated from the vorticity equation via the continuity equation and then the inconsistent quasi-geostrophic wind law, (2), adopted.

Even with these modifications, characteristic and unacceptable error patterns appeared, giving rise to the descriptive title, spurious anticyclogenesis. Shuman [17] diagnosed the malady to be due to the divergence of the advecting (i.e., geostrophic) wind which introduces vorticity sources in northerly flow and sinks in southerly flow as indicated by the closed region integral of the vorticity equation

$$\iint \frac{\partial \eta}{\partial t}\, dS = -\iint \beta f^{-1} \eta v_g dS. \tag{8}$$

Experiments at NMC [9, 17] seemed to confirm this diagnosis since all of the nondivergent wind laws B, L, and Q gave marked improvement over G (in those cases in which spurious anticyclogenesis was a problem) and B led to a much less marked improvement over L. The wind law Q was reported to have suppressed spurious anticyclogenesis slightly more than L (in at least one case), the main difference being that Q produced a slightly weaker belt of westerlies. Unfortunately no statistics were presented.

Charasch [8] postulated that the quasi-geostrophic vorticity introduced a serious error in the barotropic transformation of energy between the mean flow and the disturbances. It is equivalent to dropping the second term in his linearized expression for the rate of change of the kinetic energy of the disturbances.

$$\frac{\partial K_D}{\partial t} \sim \int_0^D \overline{u'v'}\,\overline{\zeta_G} dy + \int_0^D \overline{u'v'}\,\frac{\beta \bar{u}_g}{f}\, dy. \tag{9}$$

(The bar denotes an east-west average over the wavelength of the disturbance.) Thus the error will be greatest when the basic current is strong, the latitudinal extent, D, of the disturbance is great and in low latitudes. Bring and Charasch [4], making experimental barotropic forecasts with wind laws G, L, and B, obtained the same results as Shuman [17] but failed to establish whether the improvement was due to the use of a nondivergent wind or the more accurate vorticity field. Shuman's [17] results with Q suggest the improvement was due to the nondivergent wind.

As suggested by its name, spurious anticyclogenesis becomes severe only occasionally and is disastrous only in terms of anticyclogenesis. Because of the latter characteristic its growth can be partially controlled by placing a lower bound on the vorticity. Some numerical investigators, including FNWF (the Fleet Numerical Weather Facility at Monterey), continue to use the quasi-geostrophic wind law. According to Hughes [12] FNWF imposes a vorticity limiter (absolute vorticity greater than one-third the Coriolis parameter) in analysis of initial data and at 6-hr. intervals during the forecast. In addition, in computing the advection wind, $\sin \phi$ is replaced by $9(1+\sin\phi)^2/64+7\sin\phi)/16$ to avoid practical difficulties due to ϕ vanishing at the Equator.

3. THE POOR MAN'S BALANCE EQUATION, P

Most investigators have turned to wind laws providing a nondivergent wind field. The simplest of these is, P, the so called poor man's balance equation, (3). This wind field is nondivergent but departs systematically from the geostrophic (and therefore from the true wind) at latitudes removed from the mean latitude f_0. See figure 1. Note that a wind law is used to relate wind and pressure only within the forecast model. Once a prognostic pressure height field is produced one is free to evaluate a forecast wind by any means available.

If P is used reversibly in a forecast model to produce forecasts of pressure height it is only in the nonlinearity of the prognostic equations that an effect occurs, mainly reduced phase speeds in low latitudes and enhanced phase speeds in high latitudes. This effect is small compared to the residual errors in the prognoses. The advantages of nondivergence, fair accuracy, and ease of computation make P attractive for theoretical investigations. It was used operationally by the USAF Global Weather Central at Omaha in the 4-level model introduced in 1961.

4. THE BALANCE EQUATION, B

Despite their advantages and relative ease of computation the wind laws Q and L found few early users. Usage of L has shown a slow but steady increase particularly by those making theoretical investigations and computing the energetics of the atmosphere from actual data. The USAF Global Weather Central's 6-level model introduced in 1965 uses the L wind law.

Most investigators not satisfied with G or P have turned to B, the balance equation, (4). Because of its greater generality, the balance equation is more intellectually satisfying and appears to have gained wide acceptance for this reason alone. Shuman [17], Cressman and Hubert [9], and Bring and Charasch [4] all reported that B led to only slightly better barotropic forecasts than L.

At present the advantages of B are more difficult to demonstrate than its disadvantages, namely, the ellipticity problem encountered in solving (4) and the amount of computation time required. The blind spot or conspiracy associated with the operational use of the balance equation was recently perpetuated by Asselin [2]; he reported

TABLE 1.—*Maximum changes in pressure height required to satisfy the balance equation ellipticity criterion*

Maximum height change	Level (mb.)	Source
15 m	500	Bolin [3]
150 ft.	600	Bushby and Huckle [7]
50 ft.	500	Shuman [17]
Comparable to errors in observation and analysis	500	Arnason [1]
105 to 231 ft.	500	Author, B_1
(−69, +23) to (−181, +19) ft.	500	Author, B_2
231 to 417 ft.	300	Author, B_1
(−200, +57) to (−263, +37) ft.	300	Author, B_2

nothing concerning the magnitude of the modifications of the pressure height field required to satisfy the ellipticity criterion. Table 1 lists the maximum modification which could be found in the literature. These may be seen to contrast strongly with those found by the author using NMC balance equation programs.

The value in table 1 reported by Bushby and Huckle [7] deserves comment for two reasons. First, it is the largest of those reported in the literature although for a level and area such that it should have been the smallest. Second, it is not a modification but the difference between the initial height field and the one obtained by first solving and then inverting (4). Bushby and Huckle did not ellipticize the height field but rather, in the relaxation, replaced all negative discriminants by zero. While not reported in the literature, this procedure frees the inverted from the initial height field so that it floats tethered only at the lateral boundary. On the other hand, by satisfying the ellipticity condition before relaxing, the inverted height can be made to approach the initial as closely as desired outside the ellipticized areas.

Since introduction of the octagonal grid in 1958, NMC has used two sets of programs for solving and inverting (4). The first is essentially that described by Shuman [17]. This program set (and the stream function produced by it) has been designated B_1. The second program set, B_2, was initiated in 1963. It differs from the first in including metric terms, in using 9-point versus 3-point finite difference operators for most derivatives and in the ellipticizing procedure. In B_2 the latter is performed both times on the original height field. Initially the sum of the Laplacian of height and half the square of the Coriolis parameter are rendered nonnegative. In the second pass after eight cycles the beta and metric terms computed from the current guess of the stream function are added to the discriminant. According to Shuman (unpublished) the impetus for developing B_2 was the pressure height changes of up to 600 ft. at 300 mb. being made by B_1 to satisfy the ellipticity criterion.

Some years before this study the author modified B_1 to perform the B_2 ellipticizing procedure followed late in the relaxation by one or more passes in which both the beta term and deformation terms computed from the current guess were included before modifying the initial height to render the total discriminant nonnegative. On the 500-mb. test map a maximum change of 228 ft. was reduced to 208 ft. with addition of the beta term and 138 ft. when both beta and deformation terms were used. This suggests that B_2 might be further improved by a third ellipticizing pass which included the deformation term in the discriminant. The Laplacian of height can be increased by raising surrounding heights as well as by lowering the central height. This approach was tested using various weighting factors for the center and surrounding points. Maximum height falls were of course reduced but at the cost of slower convergence and with no improvement in distortions to the local wind field, see B_1 curve below 20°N. in figure 1.

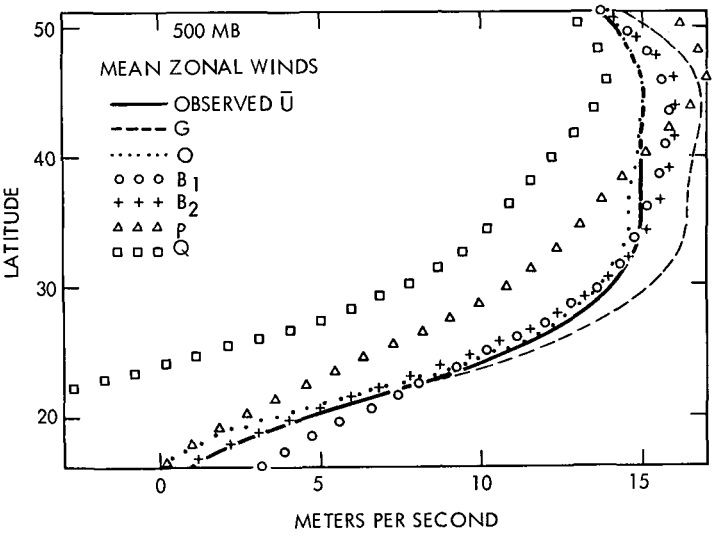

FIGURE 1.—Observed and specified mean zonal wind profiles at 500 mb. averaged over the 13 map times 0000 GMT, Nov. 29 to 0000 GMT Dec. 6, 1962 (m./sec.).

The author used both B_1 and B_2 to balance the 16 NMC pressure height analyses for the WMO NWP Test Data. The stream fields were then inverted with the appropriate program and the initial height field subtracted from the inverted one. Averages of the mean, root mean square, and standard deviations of these differences are given in table 2. These figures do not appear large because they are averages from the complete grid and only a small proportion of the points on any map are hyperbolic. The maximum difference for each map was also recorded and the smallest and largest of these are given in table 1. Both B_1 and B_2 satisfy the ellipticity criterion by lowering heights in the hyperbolic areas. Inversion of B_1 recovers the initial heights to within a few feet outside these areas so the tabulated differences are essentially height decreases made in satisfying the ellipticity criterion. Inversion of B_2 has the effect of adding a positive pillow to the ellipticized height field which reduces the negative differences in the ellipticized areas and introduces positive differences outside these areas. The two cases showing the smallest and largest maximum range between positive and negative centers are given in table 1.

For both B_1 and B_2 all the difference maps described above were combined by taking the mean of the absolute values at each grid point. These are shown for 300 mb. in figures 2 and 3 on the NMC octagon grid with the 80th meridian bisecting the lower half of the grid. Figure 2 obtained using B_1 shows the typical pattern of differences confined mainly to the subtropics and largest in the western Pacific where a mean change of 310 ft. is shown. Figure 3 shows that B_2 reduced this to 170 ft. and introduced a positive pillow of 30 to 50 ft. over most of the map. Maximum mean changes at 500 mb. were 120 and 70 ft. respectively. The more intense changes at 300 mb. were used in figures 2 and 3 to more vividly portray the problem.

According to Platzman [16], Fjørtoft [12] discovered that mixed type equations such as the balance equation can be solved by conventional relaxation methods provided only that the sign of the relaxation factor is alternated from one iteration to the next. This would appear to eliminate the ellipticity problem described above but according to André Robert (unpublished) the convergence rate of Fjørtoft's method is so slow as to make it impractical for operational use.

Thus elimination of one disadvantage of the balance equation aggravates the other, i.e., it increases the computation time. Table 3 shows the computation times for solving the balance equation quoted in the literature and found by the author for B_1 and B_2. For comparison, computation time for evaluation and inversion of the other stream functions were as follows (G and P required no computation of course): B_1, B_2 inversion 7–18 sec.; O solution 18–22 sec.; Q and L solution or inversion 7–10 sec.

The ellipticity problem of B is aggravated by strong anticyclonic relative vorticity and small Coriolis parameter; these conspire to remove the areas in which the

TABLE 2.—*Average of mean, root mean square, and standard deviation of 16 maps of difference between the inversion of B, the balance equation stream field, and initial pressure height*

Mean (ft.)	Root mean square (ft.)	Standard deviation (ft.)	Level (mb.)	Program
−9	27	25	500	B_1
2	21	20	500	B_2
−40	84	73	300	B_1
8	56	54	300	B_2

TABLE 3.—*Computation time for solving the balance equation at one data level*

Time (min.)	Data (mb.)	Number of grid points	Computer	Source
40	500	504	Swedish Besk	Bolin [3]
30	600, 500	252	Ferranti Mark I	Bushby and Huckle [7]
18	500	1020	IBM 701	Shuman [17]
1	1000, 850	1709	CDC G–20	Asselin [2]
1.7	500	1709	CDC G–20	Asselin [2]
3 to 4	200	1709	CDC G–20	Asselin [2]
1.7 to 2.6	500	1977	IBM 7094	Author, B_1
1.8 to 4.0	300	1977	IBM 7094	Author, B_1
2.5 to 4.0	500	1977	IBM 7094	Author, B_2
3.5 to 4.1	300	1977	IBM 7094	Author, B_2

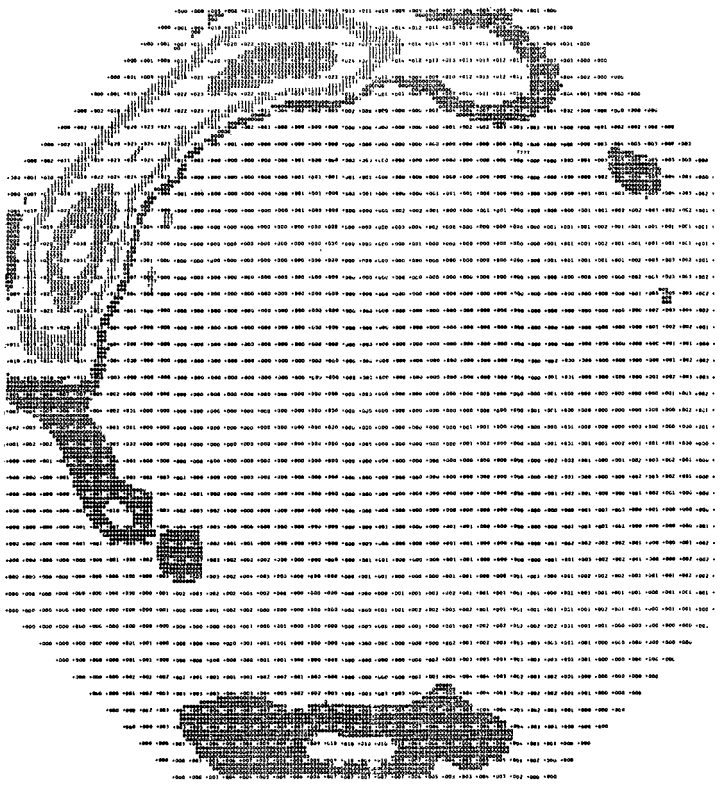

FIGURE 2.—Mean of 13 maps of difference between inversion of the stream function B_1 and the observed pressure height at 300 mb. Projection is the NMC polar sterographic octagon with 80th meridian bisecting the lower boundary. Values are in tens of feet and the contour interval is 50 ft.

FIGURE 3.—Same as figure 2 except for B_2.

problem is most severe from those of good data coverage. This consequence is frequently quoted as a reason for downgrading the problem. The author will admit that if data and ellipticity are considered simultaneously hyperbolic areas can be greatly reduced but this is not the procedure which has been followed. The NMC analysis guess fields for this test were inverted forecast B_1 fields and therefore were everywhere elliptic. Since the guess is modified only by data it is not clear how the analysis could have rendered them hyperbolic in the absence of data. Finally it appears unlikely that NMC would accept figures 2, 3, 6, and 7 as indicative of the mean error in their analysis routine for this period.

It has been suggested that use of wind laws other than B in a primitive equation model would introduce unacceptable gravity waves particularly around low centers. The author is unaware of any experiments which might help clarify this problem. However, it is deemed unlikely that the differences between gradient and geostrophic flow could compete with the differences between B and G winds indicated in table 5 in the generation of gravity waves.

5. SOLENOIDAL COMPONENT OF THE OBSERVED WIND, O

Some investigators have sought to circumvent part of the wind law problem by computing a stream function, O, directly from the observed winds by relaxing (7). Phillips [15] reported excellent results on the Thanksgiving Day Appalachian Storm of 1950 with a 2-level model using at each level a stream function obtained primarily in this way. Unfortunately NMC was unable to reproduce his results.

According to the definition of wind law, (7) must be supplemented by an equation for evaluating pressure height from the forecast stream function. I have used B and L and designated the observed stream functions as O_B and O_L, respectively.

Brown and Neilon [5] at NMC interpolated winds from O and B grid values for comparison with station observed winds at 500 mb. They found for the initial and for the 12-, 24-, and 36-hr. barotropic stream function forecasts that the O winds are the best estimates of the observed wind vectors: 13 to 25 percent smaller vector deviation. They also inverted the initial O_B and B_1 (in my notation) fields and compared them with the station observed heights. For two winter maps they obtained from B_1 root mean square differences of 44 and 71 ft. Unless the area of comparison included areas in which (4) was hyperbolic (unlikely since only station observations over United States and Canada were used) the figures should represent only errors of the analysis routine, interpolation and round-off error. For the O_B field the differences were 81 and 105 ft.

Burtsev and Vetlov [6] evaluated O from 700-mb. RAWIN data for February 1–5, 1960 on a 300-km. grid with 117 interior points. The mean vector difference between the O and observed winds was 3 m./sec. compared to 3.5 m./sec. between G and observed and 2.62 m./sec. between the vector sum of the computed fields of solenoidal (O) and potential components and the observed wind. They also expressed (4) and (5) in terms of u- and v-components and using analyses of observed winds inverted B and L to obtain the pressure height. Mean differences between the computed and observed heights were 15 m. for B, 19 m. for L.

6. COMPARISON OF WIND LAWS AT INITIAL TIME

The NMC analyses include the grid u- and v-components of the observed wind field providing a standard for evaluating the winds specified by the various wind laws. Specified mean zonal wind profiles are shown in figure 1 (L is not included since it is indistinguishable from G on this scale. Because it was uninteresting, the portion of this figure north of 50°N. was omitted to achieve scale magnification for the remainder). Maps of differences between specified and observed winds were prepared in terms of both zonal component and total vector.

The results averaged over the 13 maps used as initial data appear in tables 4 and 5 and figures 4 through 7. Because of the small difference between O, G, and L only L is reproduced in these figures. In comparing these results it should be born in mind that the winds from O differ from the observed winds only due to truncation error in computing the forcing function and relaxing (7) and in computing gradients to recover the winds. In all cases shown stream function gradients were computed using two terms of the Taylor series and four grid points along each axis. The winds from G have a definite favorable bias since the pressure height analysis and the geostrophic wind equation essentially determine the observed wind analysis in regions of few data. Also the NMC analysis program at that time multiplied observed wind speeds by 1.08 before computing height gradients from the geostrophic equation. This accounts for the algebraic mean zonal wind error of the O winds relative to all of the other winds which are evaluated from the pressure height analyses (see fig. 1).

Figures 4 through 7 show rather large differences around the boundaries (the reason for omitting two boundary rows in table 4). This is due to the general weakening of geostrophic control in low latitudes and to

TABLE 4.—*Average over 13 maps (two border rows omitted) of specified minus observed (NMC analysis) winds for the wind laws listed*

Wind law	500 mb.			300 mb.		
	Mean zonal (m./sec.)	Root mean square zonal (m./sec.)	Root mean square vector (m./sec.)	Mean zonal (m./sec.)	Root mean square zonal (m./sec.)	Root mean square vector (m./sec.)
O	−0.40	1.37	1.96	−0.05	2.24	3.34
G	0.69	1.70	2.06	0.50	2.02	2.59
L	0.64	1.72	2.28	0.37	2.20	3.29
B_2	−0.06	1.91	2.47	−1.09	4.16	5.06
B_1	0.26	2.14	2.67	−0.20	5.75	6.63
P	−0.86	3.51	4.10	−3.01	6.76	7.50
Q	−5.26	6.97	7.18	Not computed		
$G(B_1^{-1})$	0.80	2.13	2.49	1.03	5.08	5.46
$G(B_2^{-1})$	0.59	1.91	2.28	0.28	3.50	3.93

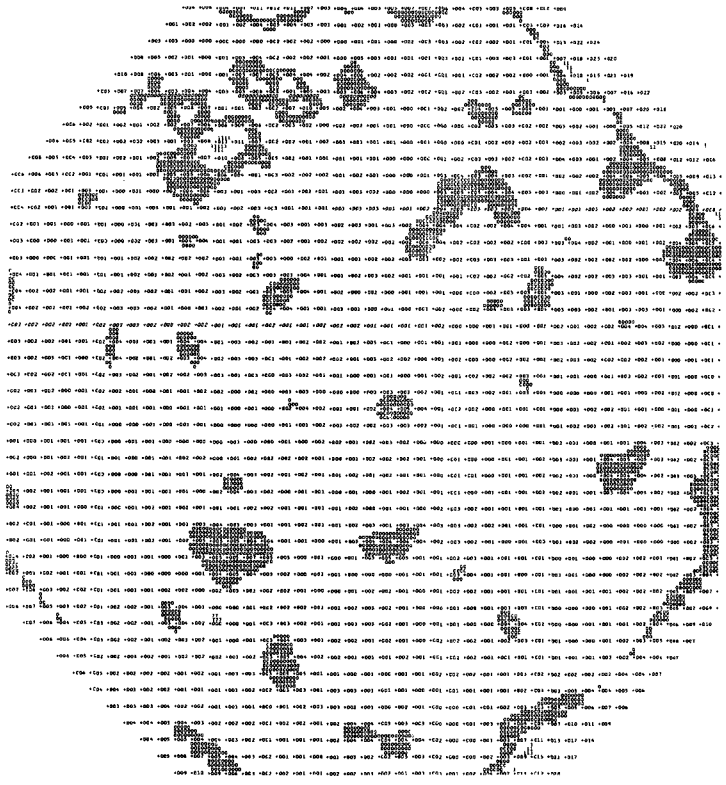

FIGURE 4.—Mean of 13 maps of vector difference between observed winds and those specified from L at 300 mb. Units are m./sec. (truncated) and contour interval is 4 m./sec. Projection as in figure 2.

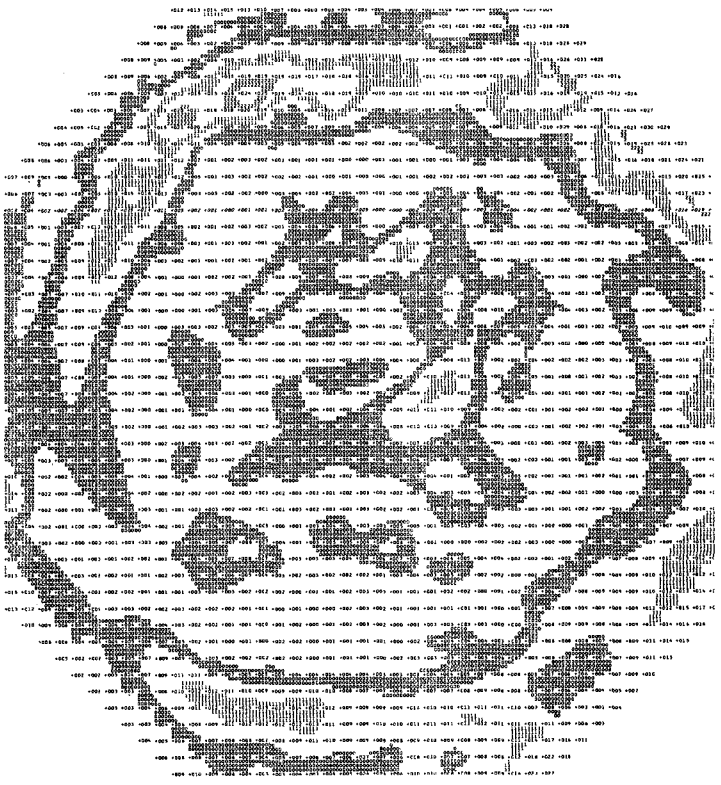

FIGURE 5.—Same as figure 4 except specified winds from P.

TABLE 5.—*Extreme values of mean error in the zonal component of the wind for each wind law. As an indication of the percentage error; $\bar{u}$, the mean zonal component of the observed wind for the point in question, is also given (m.p.s.). It is possible for these values which were rounded to exceed the vector values on figures 4 through 7 which were truncated.*

Wind law	500 mb.		300 mb.	
	Mean zonal error (m./sec.)	$\bar{u}$ (m./sec.)	Mean zonal error (m./sec.)	$\bar{u}$ (m./sec.)
O	+4	35	+7	60
G	+7	32	+16	61
L	+6	35	+13	61
B_2	−10	38	−25	61
B_1	−11	36	−28	68
P	−12	30	−25	68

the use of P as the boundary condition for all of the wind laws requiring relaxations; including O (this was the only change made in the program developed and described by Brown and Neilon [5]). Next they show that as expected the largest errors are associated with the strongest jet stream in the western Pacific.

Table 5 lists the extreme values from the maps of mean errors in the zonal component of the wind for each wind law and the average value of the zonal component of the observed wind at the corresponding point. Extreme errors of O, G, and L are positive while those of B_1, B_2, and P are negative. For 13 consecutive maps the mean jet stream at 300 mb. was (in places) 70 percent stronger than indicated by the balance equation.

Figure 1 and table 4 make it clear that Q is a very poor wind law and should definitely not be used to evaluate winds from pressure heights. The evaluation for P is not much better. One would not on theoretical grounds reject B as a source of wind for operational use. Yet such use at 300 mb. is difficult to defend after examining figures 6 and 7 which do not differ significantly in the region of the jet stream from figure 5 for P.

The large loss of kinetic energy shown by these figures is due to the combined action of satisfying the ellipticity criterion and the nonlinear term of the balance equation. In regions of strong anticyclonic shear this term is either very sensitive to the effects of ellipticizing or it is incapable of reproducing high wind speeds from a pressure height analysis biased toward geostrophic gradients. However, any attempts to strengthen the gradients or increase the anticyclonic curvature or shear are likely to be nullified in satisfying the ellipticity criterion.

That the error is not due to ellipticizing and truncation alone is shown by the data in table 4 for $G(B_1^{-1})$ (geostrophic wind computed from inversion of the B_1 field) and $G(B_2^{-1})$.

7. COMPARISON OF FORECAST PRESSURE HEIGHT

The forecasts for wind law comparisons were made on the NMC grid using a barotropic model containing

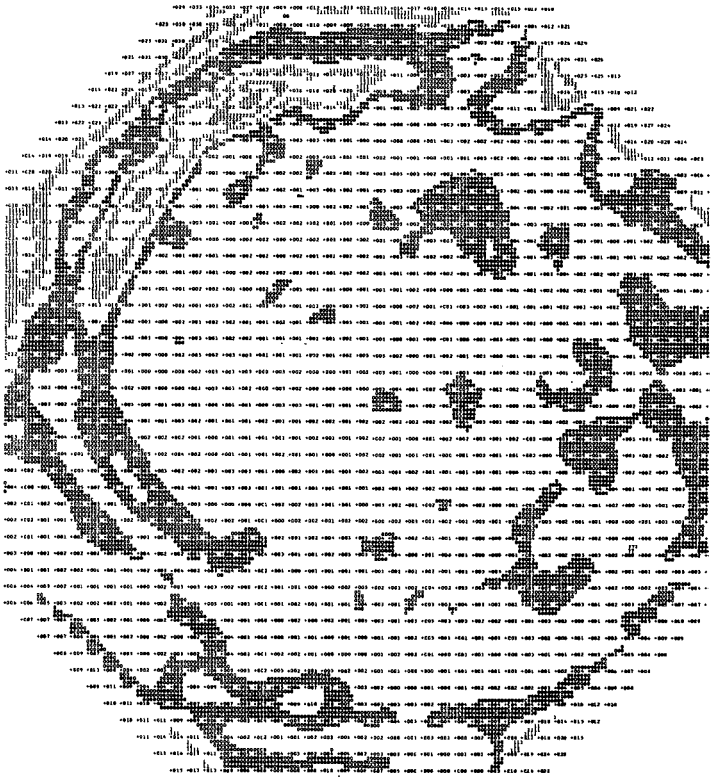

FIGURE 6.—Same as figure 4 except specified winds from B_1.

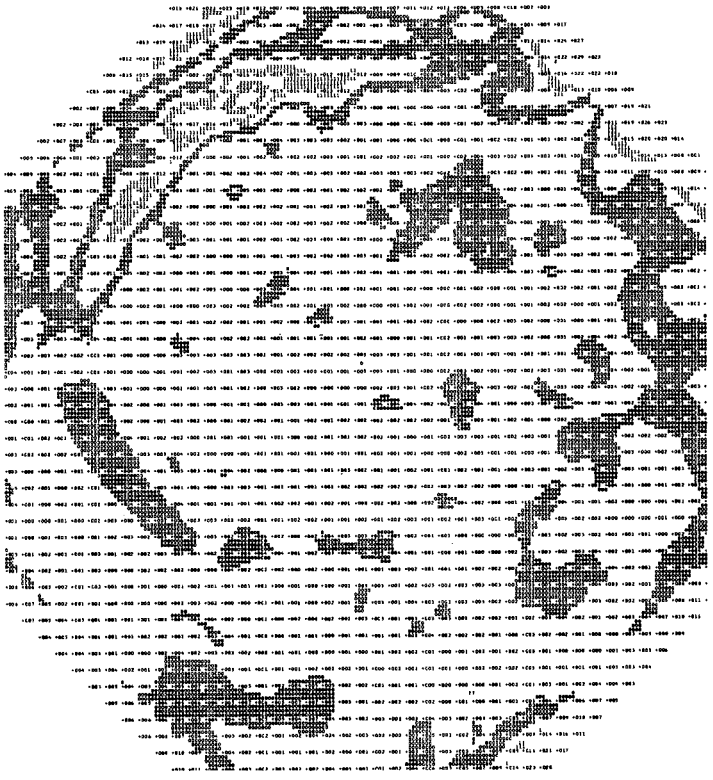

FIGURE 7.—Same as figure 4 except specified winds from B_2.

TABLE 6.—*Average (over 13 maps) of mean and standard errors in 12-, 24-, and 36-hr. barotropic forecasts of 500-mb. pressure height using wind laws indicated*

Wind law	Mean error			Standard error		
	12-hr. (ft.)	24-hr. (ft.)	36-hr. (ft.)	12-hr. (ft.)	24-hr. (ft.)	36-hr. (ft.)
NMC (opnl)			10			178
L	5	8	9	98	142	187
B_2	−8	−3	0	97	142	188
L_E	6	10	11	99	143	188
O_B	−10	−4	−4	113	150	190
O_L	48	51	53	118	155	193
G	5	8	10	102	152	202
P	5	8	10	102	153	205
Q	0	1	1	105	159	209

Helmholtz, mountain, and friction terms similar (except ΔP in denominator held constant) to those of the NMC mesh model described by Fawcett [11]. However, the model uses 600-mb. data (0.85×500 mb.) and contains no smoothing and no truncation control devices except that when the absolute vorticity becomes negative it is replaced by zero.

Table 6 contains pressure height verification data averaged over the 13 map times which could be verified to 36 hr. Standard deviations about the mean error (rather than rms) were used since mean height error is generally of little meteorological significance.

NMC operational 36-h. 500-mb. forecasts were included on the data tape and were processed by the same verification routine to obtain the values given in line 1 of table 6. These used the operational analyses as input data as opposed to the reanalyses with later data on the WMO NWP Test Data Tape used in this study. Difficult though it is to justify, still the conclusion seemed inescapable that the operational analyses generally gave the NMC forecasts a definite advantage. Other sources of differences are the 12-hr. smoothing, stronger mountain and friction terms, use of 500 mb. versus 600 mb. as the model level, and enhancement of the advection term by 13 percent in the NMC model. NMC also was using the B_1 balance equation in late 1962.

As background for interpreting the results of this comparison recall that only G has the fictitious vorticity sources and sinks represented by (8). Equatorward of the jet stream where spurious anticyclogenesis is a problem, we see from figure 1 that G, P, and Q specify rather different zonal velocities. P should forecast erroneously low phase speeds and Q even lower (possibly moving disturbance to the west rather than the east). Q should also exaggerate the problem of lagging troughs. Both G and Q use quasi-geostrophic vorticity, $\bar{\zeta}_G$ being represented by the shear of the Q curve in figure 1. Its magnitude is erroneously large over most of the region but is erroneously small near 25°N. where the true shear is largest. $\bar{\zeta}_P$, given by the shear of the P curve in figure 1, is too large between 32° and 45°N. and too small south of 30°N.

In applying (9) it will be simpler to ignore the quasi-geostrophic correction (last) term and simply compare the effects in the first term of winds and vorticities from the respective wind laws. To obtain a barotropic conversion

TABLE 7.—*Average mean, root mean square, and standard deviation of difference between inverted O stream function and pressure height at initial time*

Inverted by	500 mb.			300 mb.		
	Mean (ft.)	Root mean square (ft.)	Standard deviation (ft.)	Mean (ft.)	Root mean square (ft.)	Standard deviation (ft.)
B_1	−2	91	90	−38	135	127
B_2	−11	90	88	Not computed		
L	44	92	80	28	92	87

TABLE 8.—*Average number of grid points at which the computed absolute vorticity was negative (and replaced by zero) at time steps 0, 11, 23, and 35 in 13 barotropic forecasts with various wind laws*

Wind law	Time step			
	0	11	23	35
G	146	127	125	130
Q	141	122	119	127
B_2	141	118	114	122
L	118	106	107	111
O	117	112	111	116
P	1	6	12	22

of energy between a disturbance and the mean flow, the perturbation velocities, u' and v', must be correlated; i.e., the disturbance must be asymmetric or have a tilted axis (an axis of symmetry which is not parallel to the local meridian).

Since $\bar{\zeta}$ is negative in the region of interest the disturbance energy increases or decreases as $\overline{u'v'}$ is negative or positive; i.e., disturbances with asymmetries representative of NW to SE (NE to SW) axes should be amplified (damped).

Since G provided a more accurate advective wind and did not in this series appear to suffer significantly from the vorticity sources represented by (8), it is not surprising that the G forecasts were superior to both the P and the Q. Also the slight superiority of P over Q is not unexpected. A result at variance with that reported by Shuman [17] was the manifestation of spurious anticyclogenesis by Q. This was most pronounced in NW to SE oriented subtropical ridge lines with an easterly wind component. It also occurred occasionally in the lowest latitudes where little if any preexisting pattern was discernible. Since the advecting wind is nondivergent the source of the spurious anticyclogenesis must be that postulated by Charasch [8]. Exaggeration of the lagging trough malady was also noticeable with Q.

The results with O suffer from the absence of a one-to-one correspondence between wind and pressure height resulting in O producing the largest forecast errors at 12 hr. and errors comparable to the smallest at 36 hr. From the forecast errors, inversion by B_2 appears to be more accurate than inversion by L but this is contrary to the results at initial time shown in table 7. The results at initial time are of course subject to bias due to the influence of the geostrophic wind equation in the analysis routine and conversely verification scores may benefit from the greater smoothing inherent in the B_2 as opposed to the L inversion. The 300-mb. results in table 7 seem to resolve the issue in favor of O_L.

The B and L forecast results are nearly identical. Again recall that B_2 has a favorable bias in that the guess field for analysis of pressure height was the inversion of the B_1 12-hr. forecast. The L_E results again demonstrate that the effect of the B_2 ellipticizer on the *500-mb. pressure height* was not a problem *for this series.*

As absolute vorticity was computed a record was kept of the number of grid points at which negative values were replaced by zero. Table 8 gives the averages over the 13 forecasts at the initial, 11th, 23d, and 35th time steps. The results at initial time reflect what would be expected from figure 1. As shown previously (Ellsaesser [10]), fig. 5) the forecast scheme used dissipates mean squared vorticity rapidly. Since we are counting extrema the initial decrease for all wind laws except P is not unexpected. What is surprising is the comparable rates of increase by all wind laws in the last 12 hr.; B_2 shows the same absolute and a greater percentage increase than Q. The anomalous result for P may reflect that it has no place to go but up. However, it also suggests that P does not eliminate spurious anticyclogenesis but merely lowers the level from which it starts its growth. This is what one would expect on the basis of figure 2 and Charasch's [8] postulate as to the cause of spurious anticyclogenesis. In the individual forecasts P occasionally produced greater heights in subtropical anticyclones than either G or Q but the differences at 36 hr. were not serious and no distinguishing pattern could be identified.

Both individual error maps and means for the series were prepared and examined but were not sufficiently dissimilar to warrant publication. The Q mean error maps did show positive error centers over Greece and northwest India which were about 200 ft. higher than those of any of the other wind laws.

8. SUMMARY AND CONCLUSIONS

Of the wind laws tested L (defined by (5)) is the optimum. It provides a consistent easily computed, and reversible wind law providing a nondivergent wind field which is only slightly inferior to G (defined by (2)) and O (defined by (7)) in prescribing the observed initial wind and is inferior to none in barotropic predictions of pressure height. It is also superior to the balance equation in recovering the pressure height field from O.

The balance equation, B, requires an order of magnitude more computation time than any of the other wind laws. As currently solved it requires modifications of the pressure height field frequently exceeding 200 ft. at 500 mb. and occasionally exceeding 600 ft. at 300 and 200 mb. Even when these are not excessive, prescribed wind speeds in

and just equatorward of the jet stream are still significantly lower than observed or geostrophic speeds. In accuracy B is inferior to G, L, and O in prescribing initial winds and in barotropic forecasting of pressure heights it is no better than L.

The O wind law shows at 500 mb. the lowest standard deviation between prescribed and observed initial winds as should be expected since only truncation errors are involved. Barotropic short term forecasts with O suffer from the absence of a one-to-one correspondence between wind and pressure but this disadvantage is nearly overcome by 36 hr.

Q (defined by (6)) is the poorest of the wind laws tested and is not recommended for any purpose. P (defined by (3)) appears to offer a reasonable compromise between accuracy and computational effort and may be quite useful for theoretical investigations. It is not free from the problem of spurious anticyclogenesis but by reducing initial shears and slowing eddy growth rates in low latitudes it delays the onset of unacceptable errors of this type.

Prognostic errors which have been christened spurious anticyclogenesis are due to both the nondivergence of the advecting wind as reported by Shuman [17] and to disruption of the barotropic transfer of energy between the disturbance and the mean flow as postulated by Charasch [8]. The two processes, represented by (8) and (9), are not entirely independent since the development of either generally intensifies the effect of the other in models capable of both.

The findings of this investigation differ from previous investigations in several respects. Most of these differences can be attributed to the near hemispheric scope of this study and the inclusion of large areas of strong anticyclonic shear equatorward of the polar jet stream.

This study has considered only barotropic effects but these are also the dominant effects in baroclinic models. However, the results with baroclinic models will depend primarily on how kinetic energy is generated and dissipated by the model, both processes being highly scale dependent (though not in the same way) in numerical models and in the atmosphere.

9. ACKNOWLEDGMENT

The cooperation of NMC in supplying the data and many of the machine programs used in this study is gratefully acknowledged.

REFERENCES

1. G. 'Arnason, "A Convergent Method for Solving the Balance Equation," *Journal of Meteorology*, vol. 15, No. 2, Apr. 1958, pp. 220–225.
2. R. Asselin, "The Operational Solution of the Balance Equation," *Tellus*, vol. 19, No. 1, 1967, pp. 24–32.
3. B. Bolin, "An Improved Barotropic Model and Some Aspects of Using the Balance Equation for Three-Dimensional Flow," *Tellus*, vol. 8, No. 1, Feb. 1956, pp. 61–73.
4. A. Bring and E. Charasch, "An Experiment in Numerical Prediction With Two Non-geostropic Barotropic Models," *Tellus*, vol. 10, No. 1, Feb. 1958, pp. 88–94.
5. J. A. Brown and J. R. Neilon, "Case Studies of Numerical Wind Analyses," *Monthly Weather Review*, vol. 89, No. 3, Mar. 1961, pp. 83–90.
6. A. I. Burtsev and I. P. Vetlov, "Vosstanovlenie Polia Geopotentsiala po Poliu Vetra i Polia Vetra po Vikhriu i Divergentsii" [The Computation of the Geopotential Field From the Wind Field and of the Wind Field From the Vorticity and Divergence], *Meteorologiia i Gidrologiia*, Moscow, No. 5, May 1962, pp. 8–16.
7. F. H. Bushby and V. M. Huckle, "The Use of a Stream Function in a Two-Parameter Model of the Atmosphere," *Quarterly Journal of the Royal Meteorological Society*, vol. 82, No. 354, Oct. 1956, pp. 409–418.
8. E. Charasch, "Note on Numerical Prediction of Intensity Changes of Disturbances With the Aid of the Quasi-Geostrophic Barotropic Model," *Tellus*, vol. 10, No. 1, Feb. 1958, pp. 95–98.
9. G. P. Cressman and W. E. Hubert, "A Study of Numerical Forecasting Errors," *Monthly Weather Review*, vol. 85, No. 7, July 1957, pp. 235–242.
10. H. W. Ellsaesser, "Evaluation of Spectral Versus Grid Methods of Hemispheric Numerical Weather Prediction," *Journal of Applied Meteorology*, vol. 5, No. 3, June 1966, pp. 246–262.
11. E. B. Fawcett, "Six Years of Operational Numerical Weather Prediction," *Journal of Applied Meteorology*, vol. 1, No. 3, Sept. 1962, pp. 318–332.
12. R. Fjørtoft, "A Numerical Method of Solving Certain Partial Differential Equations of Second Order," *Geofysiske Publikasjoner*, Oslo, vol. 24, 1962, pp. 229–239.
13. R. E. Hughes, "Computer Products Manual," *Technical Note No. 21*, Fleet Numerical Weather Facility, Monterey, California, July 1966, various pp.
14. M. Neiburger and J. K. Angell, "Meteorological Applications of Constant-Pressure Balloon Trajectories," *Journal of Meteorology*, vol. 13, No. 2, Apr. 1956, pp. 166–194.
15. N. A. Phillips, "Geostrophic Errors in Predicting the Appalachian Storm of November 1950," *Geophisica*, Helsinki, vol. 6, No. 3/4, 1958, pp. 389–405.
16. G. W. Platzman, "International Symposium on Numerical Weather Forecasting, Oslo, March 11–16, 1963," *Tellus*, vol. 15, No. 3, Aug. 1963, pp. 284–286.
17. F. G. Shuman, "Predictive Consequences of Certain Physical Inconsistencies in the Geostrophic Barotropic Model," *Monthly Weather Review*, vol. 85, No. 7, July 1957, pp. 229–234.

[Received September 21, 1967; revised March 5, 1968]

295-999 O - 68 - 3